arXiv:1408.3509v3 [cond-mat.mes-hall] 17 Dec 2014

Topological tuning in three-dimensional Dirac semimetals

Awadhesh Narayan*
School of Physics and CRANN, Trinity College, Dublin 2, Ireland

Domenico Di Sante†
Consiglio Nazionale delle Ricerche (CNR-SPIN), Via Vetoio, L'Aquila, Italy and
Department of Physical and Chemical Sciences, University of L'Aquila, Via Vetoio 10, I-67010 L'Aquila, Italy

Silvia Picozzi
Consiglio Nazionale delle Ricerche (CNR-SPIN), Via Vetoio, L'Aquila, Italy

Stefano Sanvito
School of Physics, CRANN and AMBER, Trinity College, Dublin 2, Ireland

(Dated: December 18, 2014)

We study with first-principles methods the interplay between bulk and surface Dirac fermions in three dimensional Dirac semimetals. By combining density functional theory with the coherent potential approximation, we reveal a topological phase transition in $Na_3Bi_{1-x}Sb_x$and $Cd_3[As_{1-x}P_x]_2$ alloys, where the material goes from a Dirac semimetal to a trivial insulator upon changing Sb or P concentrations. Tuning the composition allows us to engineer the position of the bulk Dirac points in reciprocal space. Interestingly, the phase transition coincides with the reversal of the band ordering between the conduction and valence bands.

Introduction. In recent years an ever growing attention has been devoted to Dirac fermions, both in two as well as in three dimensions. The fabrication of graphene and topological insulators has motivated a surge of investigations in this field [1–3]. Acting as a possible bridge between the two, recently Dirac semimetals in three dimensions were theoretically proposed [4]. Using first-principles calculations, Wang and co-workers predicted sodium bismuthate (Na_3Bi) and cadmium arsenide (Cd_3As_2) to be three dimensional Dirac semimetals [5, 6]. Their experimental realization has not been far behind and the prediction verified by means of angle resolved photoemission measurements in a remarkably rapid flurry of activity by a number of groups [7–11]. Interestingly, a Dirac semimetal state was also found in zinc blende compounds [12]. Apart from hosting a bulk Dirac cone, both Na_3Bi and Cd_3As_2 also show a band inversion at the center of the Brillouin zone (BZ). This means that they exhibit a surface Dirac spectrum when confined to a slab geometry, analogously to conventional topological insulators [13]. Given their unique electronic structure, these class of compounds opens up an exciting platform to study topological phase transitions, interweaving two and three dimensional Dirac states.

In this Letter we study the interplay of surface and bulk Dirac states by using first-principles density functional theory (DFT) and *ab-initio*-derived tight-binding models. Based on our first-principles calculations, we predict that the bulk Dirac cone of Na_3Bi is formed only for films with a thickness larger than 90 nm, while the surface Dirac state, originating from a bulk band inversion, becomes gapless for films with a thickness as small as 4.5 nm, up to an energy resolution of ≈ 3 meV (a resolution accessible by the most recent state-of-the-art spectrometers [14]). Furthermore, by employing the coherent potential approximation joint with DFT, we uncover a topological phase transition in the $Na_3Bi_{1-x}Sb_x$ and $Cd_3[As_{1-x}P_x]_2$ alloys. We propose a means to engineer the k-space position of the bulk Dirac point by changing the Sb or P concentrations. At the critical Sb (P) concentration of $\approx 50\%$ ($\approx 10\%$), this crossing reaches the BZ center, meeting its time-reversed partner, whereupon they annihilate and render the bulk gapped. This topological phase transition is accompanied by a simultaneous loss of the inverted band character. Beyond the critical Sb (P) concentration, the alloy is adiabatically connected to the topologically trivial Na_3Sb (Cd_3P_2).

Computational Methods. We have carried out first-principles calculations by using the projector augmented

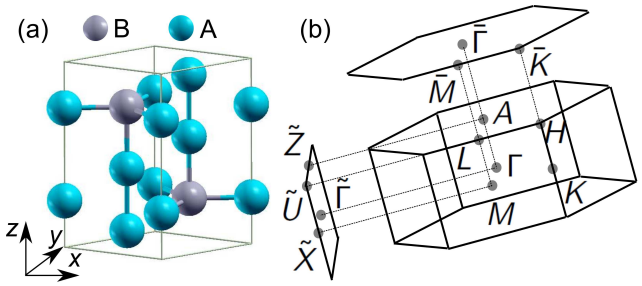

FIG. 1: (Color online) (a) Hexagonal unit cell for A_3B compounds, with A=Na, K, Rb and B=Bi, Sb. (b) Bulk and surface projected Brillouin zone for the structure with the high symmetry points marked. The three dimensional Dirac crossing occurs along the $\Gamma - A$ direction.

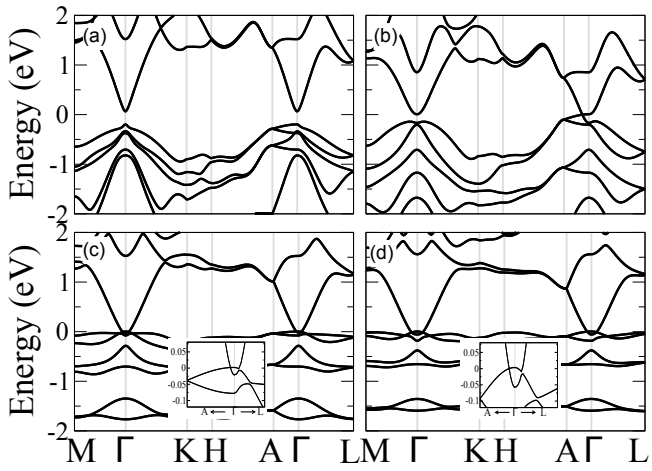

FIG. 2: Bulk band structures obtained by including spin orbit interaction for (a) Na_3Sb, (b) Na_3Bi, (c) K_3Bi and (d) Rb_3Bi. Note the Dirac crossing in (b)-(d). The insets in (c) and (d) show a zoom around Γ with the crossing along $\Gamma - A$.

plane wave method as implemented in Vienna Ab-initio Simulation Package (VASP) [15], and employed the Perdew-Burke-Ernzerhof parameterization of the exchange-correlation functional [16]. Spin orbit coupling was included for all computations in a self-consistent manner. The electronic structure simulations have been performed with a plane wave cutoff of 600 eV on a 8×8×4 Monkhorst-Pack k-point mesh. All the A_3B compounds (A=Na, K, Rb, B=Bi, Sb) investigated here crystallize in the D^4_{6h} structure, as shown in Fig. 1. During the structural optimization the atomic coordinates were allowed to relax until total energy differences were less than 1 meV. From the bulk first-principles results, we have projected onto a basis of Na 3s and Bi 6p (Sb 5p) orbitals by using a procedure based on constructing Wannier functions [17]. The obtained tight-binding parameters were then used to study slab geometries. By combining this scheme with a coherent potential approximation (CPA) including self-energy corrections for disorder, we have investigated the $Na_3Bi_{1-x}Sb_x$ alloy [18]. We note that this methodology has been recently used to predict the robustness of Dirac fermions in Topological Crystalline Insulator (TCI) alloys, as well as in Ferroelectric Rashba Semiconductor (FERSC) alloys [19].

Results and discussions. We begin our analysis by calculating the relativistic bulk band structures for the four materials Na_3Sb, Na_3Bi, K_3Bi and Rb_3Bi, as shown in Fig. 2. For Na_3Bi we find the three dimensional Dirac crossing along the $\Gamma - A$ line, and a band inversion at the BZ center, which is consistent with the previous study of Wang *et al.* [5]. Na_3Sb, in contrast, is a small gap insulator with a conventional band ordering. Our calculations reveal that on replacing Na in Na_3Bi with heavier atoms, the resulting compounds K_3Bi and Rb_3Bi are metallic with small electron pockets around Γ. However the crossing away from Γ is still present. The band structures for the two materials are shown in Fig. 2(c) and (d), along with a zoom around the BZ center in the insets. A transition from a hexagonal to a cubic form has been reported for K_3Bi and Rb_3Bi at high temperatures [20, 21]. So, our results for the band structures of these two materials are expected to hold at low temperatures.

Since Na_3Bi also shows an inverted band character around the Fermi level, one expects it to form surface states when confined into a two-dimensional geometry, similar to a topological insulator. Therefore, we study the evolution of the spectrum of Na_3Bi films oriented along the [010] surface, as a function of their thickness. For thicknesses ranging from 1 to 4 layers, the films are gapped due to an interaction between the two surfaces, as shown in Fig. 3(a). This gap decreases monotonically, with the surface cone at $\widetilde{\Gamma}$ becoming gapless for a 5-layer-thick film. One can also notice the shoulder along the $\widetilde{\Gamma} - \widetilde{Z}$ direction, which rises upwards in energy to form the bulk Dirac crossing for thicker films. This bulk crossing is fully formed only for film thicknesses larger than 100 layers (≈ 90 nm). We note that the Fermi arcs can exist with the bulk Dirac nodes, as long as the two-dimensional $\mathbb{Z}_2$ invariant on the $k_z = 0$ plane, ν_{2D}, is non-trivial [22]. Our predictions for the thickness dependence of the surface and bulk Dirac cones call for verifications by angle resolved photoemission experiments. Indeed, such measurements with varying film thickness have been recently undertaken for topological insulator films [23, 24]. In the case of Na_3Bi [010] slabs, one should be able to see two

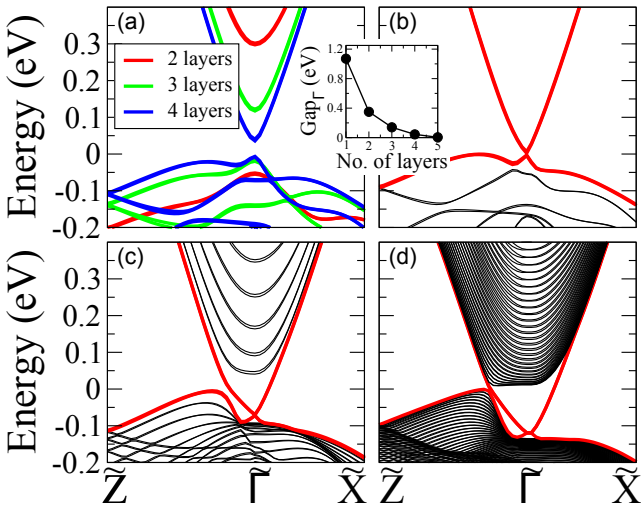

FIG. 3: (Color online) Band structures for Na_3Bi thin films of thickness (a) 2-4 layers, (b) 5 layers, (c) 20 layers and (d) 100 layers. Inset in (a)-(b) shows the energy gap at the center of the Brillouin zone for slabs of thickness 1 to 5 layers. In (b)-(d) Dirac crossings are highlighted in red.

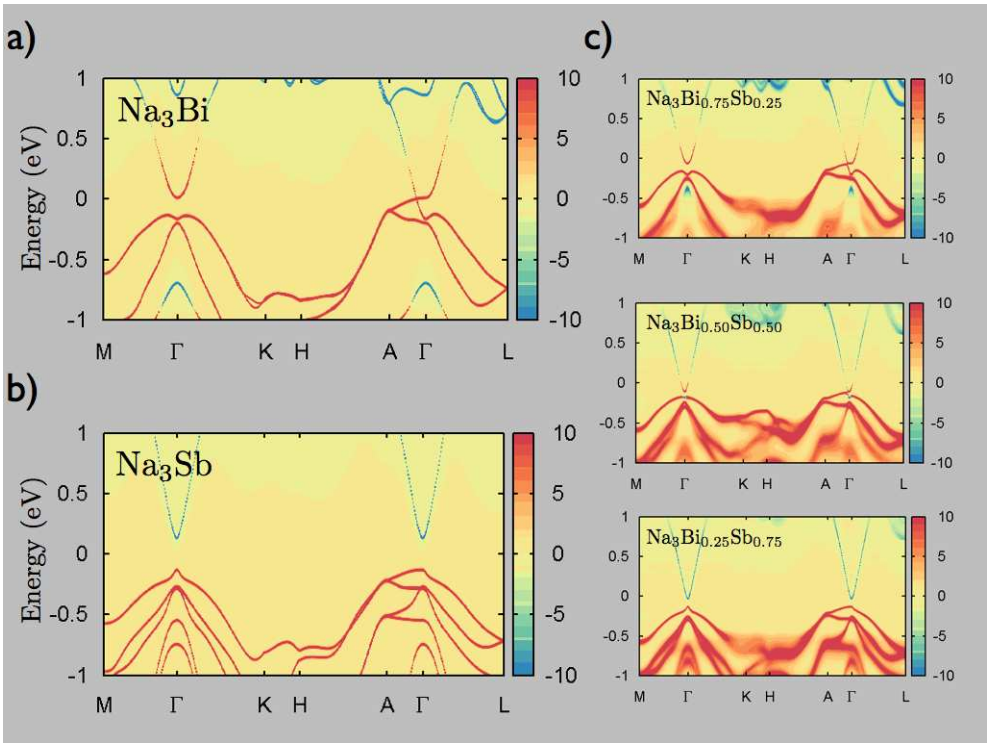

FIG. 4: (Color online) Spectral functions for pristine (a) Na_3Bi and (b) Na_3Sb. (c) Spectral functions for the $Na_3Bi_{1-x}Sb_x$ alloy with increasing Sb concentration ($x = 0.25, 0.50, 0.75$ from top to bottom). The color scale shows the orbital contribution, with red (positive values) denoting Bi/Sb p orbitals and blue (negative values) representing Na s orbital (in units of states/eV).

gap-closing transitions at very different film thicknesses: one for the surface cone for a few layers slab, with the next gap-closing occurring in the bulk for a hundred layers slab. For the [001] surface, the bulk and surface Dirac cones are all projected onto the Brillouin zone center. In contrast, these Dirac crossings are separated in reciprocal space for the [010] surface. We decided to focus on the latter, as in this case it may be easier to distinguish the two cones in a angle-resolved photoemission measurement. Very recently thin films of Na_3Bi have been grown by molecular beam epitaxy [25], a development which provides a clear route to verify our predictions.

We turn now our attention to the $Na_3Bi_{1-x}Sb_x$ alloy. From the bulk band structures in Fig. 2, we observe that Na_3Sb is topologically trivial, having neither the bulk Dirac crossing nor a band inversion at the BZ center, as opposed to Na_3Bi. This opens up the intriguing possibility to obtain a quantum phase transition in $Na_3Bi_{1-x}Sb_x$ solid solutions. To this end, we have performed DFT+CPA calculations for the alloy. The spectral functions at different Sb concentrations are shown in Fig. 4. With increasing Sb concentration, the bulk Dirac crossing along $\Gamma - A$ moves towards the BZ center. At around a critical concentration of $x_c = 0.5$ ($Na_3Bi_{0.5}Sb_{0.5}$), this crossing reaches close to Γ. Upon subsequent increase in Sb concentration, an energy gap appears. We note that this is the consequence of the annihilation between this Dirac cone and its time reversed partner along the Γ to A direction. The Sb concentration therefore represents an efficient tool to manipulate the position of the bulk Dirac points in k-space along the $\Gamma - A$ line. Interestingly, the disappearance of the bulk cone is accompanied by a loss of the inverted band character, as it can be evidenced from the reversal in orbital character of the valence and conduction bands, before and after passing through the critical Sb concentration. From bulk-boundary correspondence, one can then infer that for slabs made of these alloys there would also be a transition in the surface spectrum: below x_c the surface would display a Dirac crossing, while increasing Sb concentration beyond this value would lead to the opening of a trivial gap. Thus, our calculations reveal a topological phase transition in the prototypical three-dimensional Dirac semimetal.

Recently, such tunable phase transitions were experimentally reported for topological insulators and topological crystalline insulators [26–29]. This makes us confident that our predictions can be verified in the near future. It is also worthy considering that our DFT+CPA calculations reveal a protection against substitutional disorder of the spectral features of three-dimensional Dirac semimetals around the Fermi level. We note, in fact,

the absence of broadening of spectral features around the cone, as compared to other energies. Such a robustness, similar to what happens for topological crystalline insulators and Weyl fermion systems, arises from the three-dimensional nature of the Dirac cone [19], and in turn leads to the concrete possibility of experimental verifications by means of spectroscopic techniques. As shown in Ref. [19], this is a consequence of a vanishing disorder self-energy around the crossing point. We also propose that a similar phase transition, and a similar robustness against disorder, would occur in the $Cd_3(As_{1-x}P_x)_2$ alloy, since the parent compounds Cd_3As_2 and Cd_3P_2 are Dirac semi-metal and conventional insulator, respectively, with the former having an inverted band order and the latter having a normal band sequence (see supplemental material [30]).

Conclusions. In summary, we have studied the interplay between bulk and surface Dirac fermions in prototypical three dimensional Dirac semimetals, by using first-principles-based tight-binding calculations. Furthermore, by means of density functional theory with coherent potential approximation simulations, we have revealed a topological phase transition in $Na_3Bi_{1-x}Sb_x$and $Cd_3[As_{1-x}P_x]_2$. The change of Sb or P concentration provides an efficient way to engineer the reciprocal space position of the three dimensional Dirac cone, with potential implications for technological devices benefiting from this additional degree of freedom. Intriguingly, the phase transition from a Dirac semimetal to an insulator is accompanied by a change in the bulk band ordering. This can be related, via the bulk-boundary correspondence, to a concomitant transition in the surface state spectrum.

Acknowledgments. AN thanks the Irish Research Council (IRC) for financial support. DDS and SP thank the CARIPLO Foundation through the MAGISTER project Rif. 2013-0726. We acknowledge CINECA, Irish Centre for High-End Computing (ICHEC) and Trinity Center for High Performance Computing (TCHPC) for providing computational resources. DDS and AN thank Prof. C. Franchini for useful correspondence. DDS kindly thanks Prof. S. Ciuchi for valuable discussions about CPA calculations and disorder, and E. Plekhanov for useful cross-checkings of slab calculations.

* Electronic address: narayaa@tcd.ie
† Electronic address: domenico.disante@aquila.infn.it

[1] A.K. Geim and K.S. Novoselov, Nature Mater. **6**, 183 (2007).
[2] M.Z. Hasan and C.L. Kane, Rev. Mod. Phys. **82**, 3045 (2010).
[3] X.-L. Qi and S.-C. Zhang, Rev. Mod. Phys. **83**, 1057 (2011).
[4] S.M. Young, S. Zaheer, J.C.Y. Teo, C.L. Kane, E.J. Mele, and A.M. Rappe, Phys. Rev. Lett. **108**, 140405 (2012).
[5] Z. Wang, Y. Sun, X.-Q. Chen, C. Franchini, G. Xu, H. Weng, X. Dai, and Z. Fang, Phys. Rev. B **85**, 195320 (2012).
[6] Z. Wang, H. Weng, Q. Wu, X. Dai, and Z. Fang, Phys. Rev. B **88**, 125427 (2013).
[7] Z.K. Liu, B. Zhou, Y. Zhang, Z.J. Wang, H.M. Weng, D. Prabhakaran, S.-K. Mo, Z.X. Shen, Z. Fang, X. Dai, Z. Hussain, and Y.L. Chen, Science **343**, 864 (2014).
[8] S.-Y. Xu, C. Liu, S.K. Kushwaha, T.-R. Chang, J.W. Krizan, R. Sankar, C.M. Polley, J. Adell, T. Balasubramanian, K. Miyamoto, N. Alidoust, G. Bian, M. Neupane, I. Belopolski, H.-T. Jeng, C.-Y. Huang, W.-F. Tsai, H. Lin, F.C. Chou, T. Okuda, A. Bansil, R.J. Cava, and M.Z. Hasan, arXiv:1312.7624.
[9] Z.K. Liu, J. Jiang, B. Zhou, Z.J. Wang, Y. Zhang, H.M. Weng, D. Prabhakaran, S.-K. Mo, H. Peng, P. Dudin, T. Kim, M. Hoesch, Z. Fang, X. Dai, Z.X. Shen, D.L. Feng, Z. Hussain, and Y.L. Chen, Nature Mat. **13**, 677 (2014).
[10] M. Neupane, S.-Y. Xu, R. Sankar, N. Alidoust, G. Bian, C. Liu, I. Belopolski, T.-R. Chang, H.-T. Jeng, H. Lin, A. Bansil, F.C. Chou, and M.Z. Hasan, Nature Commun. **5**, 3786 (2014).
[11] S. Borisenko, Q. Gibson, D. Evtushinsky, V. Zabolotnyy, B. Buchner, and R.J. Cava, Phys. Rev. Lett. **113**, 027603 (2014).
[12] M. Orlita, D.M. Basko, M.S. Zholudev, F. Teppe, W. Knap, V.I. Gavrilenko, N.N. Mikhailov, S.A. Dvoretskii, P. Neugebauer, C. Faugeras, A-L. Barra, G. Martinez, and M. Potemski, Nature Phys. **10**, 233 (2014).
[13] H. Zhang, C.-X. Liu, X.-L. Qi, X. Dai, Z. Fang, and S.-C. Zhang, Nature Phys. **5**, 438 (2009).
[14] A. Damascelli, Physica Scripta. T109, **61** (2004).
[15] G. Kresse and J. Furthmuller, Comput. Mater. Sci. **6**, 15 (1996).
[16] J.P. Perdew, K. Burke, and M. Ernzerhof, Phys. Rev. Lett. **77**, 3865 (1996).
[17] A. A. Mostofi, J. R. Yates, Y.-S. Lee, I. Souza, D. Vanderbilt and N. Marzari, Comput. Phys. Commun. **178**, 685 (2008).
[18] P. Soven, Phys. Rev. **156**, 809 (1967).
[19] D. Di Sante, P. Barone, E. Plekhanov, S. Ciuchi, and S. Picozzi, arXiv:1407.2064.
[20] Sands *et al.*, J. : Acta. Crystallogr. **16**, 316 (1963).
[21] Chuntonov *et al.*, Sov. Phys. Crystallogr. **22**, 367 (1977).
[22] B.-J. Yang and N. Nagaosa, Nat. Commun. **5**, 4898 (2014).
[23] Y. Zhang *et al.*, Nature Phys. **6**, 584 (2010).
[24] M. Neupane *et al.*, Nature Commun. **5**, 3841 (2014).
[25] Y. Zhang *et al.*, Appl. Phys. Lett. **105**, 031901 (2014).
[26] S.-Y. Xu, Y. Xia, L.A. Wray, S. Jia, F. Meier, J.H. Dil, J. Osterwalder, B. Slomski, A. Bansil, H. Lin, R.J. Cava, and M.Z. Hasan, Science **332**, 560 (2011).
[27] T. Sato, K. Segawa, K. Kosaka, S. Souma, K. Nakayama, K. Eto, T. Minami, Y. Ando, and T. Takahashi, Nature Phys. **7**, 840 (2011).
[28] P. Dziawa *et al.*, Nature Mater. **11**, 1023 (2012).
[29] S.-Y. Xu *et al.*, Nature Commun. **3**, 1192 (2012).
[30] See supplemental material for CPA calculations for the $Cd_3(As_{1-x}P_x)_2$ alloy, along with a low-energy model to study the topological phase transition.

Supplemental Material: Topological tuning in three-dimensional Dirac semimetals

Awadhesh Narayan
School of Physics and CRANN, Trinity College, Dublin 2, Ireland

Domenico Di Sante
Consiglio Nazionale delle Ricerche (CNR-SPIN), Via Vetoio, L'Aquila, Italy and
Department of Physical and Chemical Sciences, University of L'Aquila, Via Vetoio 10, I-67010 L'Aquila, Italy

Silvia Picozzi
Consiglio Nazionale delle Ricerche (CNR-SPIN), Via Vetoio, L'Aquila, Italy

Stefano Sanvito
School of Physics, CRANN and AMBER, Trinity College, Dublin 2, Ireland
(Dated: October 27, 2014)

In this supplement we elaborate on (i) an alloying-induced topological phase transition in $Cd_3[P_{1-x}As_x]_2$, and (ii) a general low-energy Dirac-like Hamiltonian for three-dimensional Dirac semimetals to study this transition.

ALLOYING INDUCED TRANSITION IN $Cd_3[P_{1-x}As_x]_2$

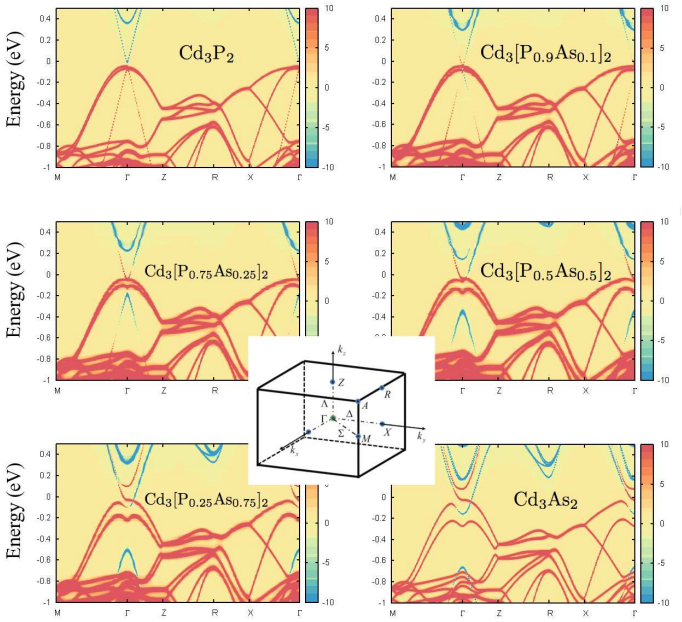

FIG. 1: Spectral functions for the alloy $Cd_3[P_{1-x}As_x]_2$ with increasing As concentration ($x = 0.0, 0.10, 0.25, 0.50, 0.75, 1.0$ from top to bottom and from left to right). The color scale shows the orbital contribution, with red (positive values) denoting P/As p orbitals and blue (negative values) representing Cd s orbitals (in units of states/eV). The central inset shows the tetragonal Brillouin zone of the $P4_2/nmc$ space group.

In addition to Na_3Bi, also Cd_3As_2 has been observed to show a three dimensional Dirac semimetal state. We predict that, analogously to $Na_3Bi_{1-x}Sb_x$ alloys, a similar topological phase transition can be observed in $Cd_3[P_{1-x}As_x]_2$. In order to study the alloying-induced topological transition in the $Cd_3[P_{1-x}As_x]_2$ alloys, we consider both pristine

compounds, i.e. Cd_3P_2 and Cd_3As_2, in their $P4_2/nmc$ space group structure [2, 3]. We note here that Cd_3As_2 has been recently predicted to crystallize at ambient conditions into the $I4_1/acd$ space group, a $\sqrt{2} \times \sqrt{2} \times 2$ supercell of the $P4_2/nmc$ structure [4]. However, low-energy features are robust against the choice of the space group, as can be inferred by comparing bandstructures reported in Refs. [2] and [4], so that we perform our simulations for the smaller $P4_2/nmc$ cell.

In Fig. 1 we report our CPA calculations for $Cd_3[P_{1-x}As_x]_2$ alloys, highlighting that Cd_3P_2 shows a trivial gap of ~ 50 meV, while in Cd_3As_2 a topological bulk band crossing occurs along the $\Gamma - Z$ line at the Fermi level. Our calculations reveal that a small concentration of As, namely $x = 0.10$, is sufficient to achieve the topological bulk gap closure. Furthermore, we note also that the low-energy features around the 3D Dirac cone are protected against the broadening action of disorder, preserving their quasiparticle nature [5], and for this reason they should be clearly detectable in angle-resolved photoemission experiments.

These results for $Cd_3[P_{1-x}As_x]_2$ alloys are analogous to those reported for $Na_3Bi_{1-x}Sb_x$ alloys, as detailed in the main manuscript. However, Na_3Bi and Na_3Sb are unstable in air and special care is needed to prepare the samples. In contrast, Cd_3As_2 and Cd_3P_2 are stable in atmosphere conditions. Moreover, Cd_3As_2 is known to have very high mobility, which we also expect the alloys to inherit.

LOW-ENERGY HAMILTONIAN AND TOPOLOGICAL PHASE TRANSITION

A minimal 4×4 low-energy Hamiltonian for the Dirac semimetal around the Brillouin zone center (Γ) can be written down as [1, 2]

$$\mathcal{H}(\mathbf{k}) = \epsilon_0(\mathbf{k})\mathbb{I} + \begin{pmatrix} M(\mathbf{k}) & Ak_+ & 0 & B^*(\mathbf{k}) \\ Ak_- & -M(\mathbf{k}) & B^*(\mathbf{k}) & 0 \\ 0 & B(\mathbf{k}) & M(\mathbf{k}) & -Ak_- \\ B(\mathbf{k}) & 0 & -Ak_+ & -M(\mathbf{k}) \end{pmatrix}, \tag{1}$$

where $\epsilon_0(\mathbf{k}) = C_0 + C_1k_z^2 + C_2(k_x^2 + k_y^2)$, $\mathbb{I}$ is a 4×4 identity matrix, $k_\pm = k_x \pm ik_y$, $M(\mathbf{k}) = m_0 - m_1k_z^2 - m_2(k_x^2 + k_y^2)$, and $B(\mathbf{k}) = B_3k_zk_+^2$. Here the basis is $[|S^+, 1/2\rangle, |P^-, 3/2\rangle, |S^-, 1/2\rangle, |P^-, 3/2\rangle]$, with S and P denoting the hybrid states from the Na and the Bi atoms, the superscript $\pm$ labels the parity and the second number in the ket vector denotes the total angular momentum. We use the following parameters for Na_3Bi, obtained by fitting to first-principles results [1]: $C_0 = -63.82$ meV, $C_1 = 8.7536$ eVÅ^2, $C_2 = -8.4008$ eVÅ^2, $m_1 = -10.6424$ eVÅ^2, $m_2 = -10.3610$ eVÅ^2, and $A = 2.4598$ eVÅ. We then tune the value of the mass parameter, m_0, to obtain the phase transition as shown in Fig. 2. The two Dirac nodes move towards the Γ point as the mass is increased (m_0 is tuned towards zero from negative values), they meet at the critical point $m_0 = 0$ and then a trivial gap opens up in the spectrum for $m_0 > 0$. This well models our density functional theory and coherent potential approximation results for $Na_3Bi_{1-x}Sb_x$ alloy presented in the main paper.

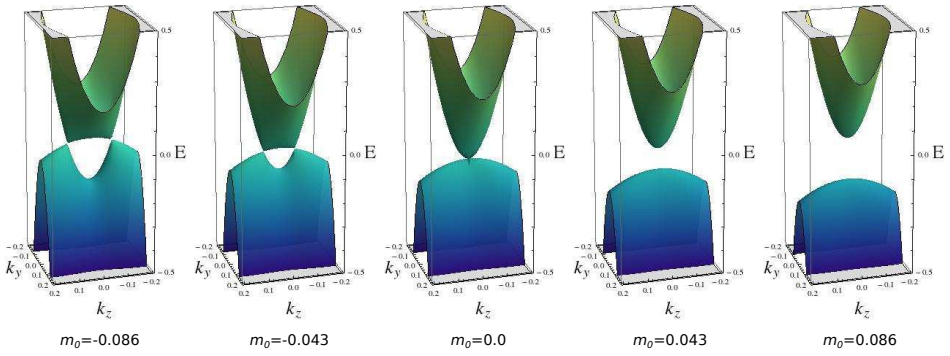

FIG. 2: Band structure for the effective low-energy Dirac model as a function of the mass term, showing the topological transition from Dirac semimetal to a trivial insulator. Note the shifting of the Dirac crossing towards Γ as the mass is increased to zero.

[1] Z. Wang, Y. Sun, X.-Q. Chen, C. Franchini, G. Xu, H. Weng, X. Dai, and Z. Fang, Phys. Rev. B **85**, 195320 (2012).
[2] Z. Wang, H. Weng, Q. Wu, X. Dai, and Z. Fang, Phys. Rev. B **88**, 125427 (2013).
[3] U. Paliwal and K.B. Joshi, Physica B **406**, 3060 (2011).
[4] M.N. Ali, Q. Gibson, S. Jeon, B.B. Zhou, A. Yazdani and R.J. Cava, Inorg. Chem. **53**, 4062 (2014).
[5] D. Di Sante, P. Barone, E. Plekhanov, S. Ciuchi, and S. Picozzi, arXiv:1407.2064.